CO-REGISTRATION AND INTER-SENSOR COMPARISON OF MODIS AND LANDSAT 7 ETM+ DATA AIMED AT NDVI CALCULATION

P Boccardo[a], E Borgogno Mondino[a], F Perez[a], P Claps[b]

[a] DITAG-Politecnico di Torino, TORINO, Italy - (piero.boccardo, enrico.borgogno, francesca.perez)@polito.it
[b] DITIC-Politecnico di Torino, TORINO, Italy – (pierluigi.claps@polito.it)

Commission I, WG I

KEY WORDS: Comparison, Integration, Registration, Landsat, Resolution, Thematic

ABSTRACT:

To evaluate accuracy of low resolution vegetation mapping for hydrological purposes, a comparative study of NDVI images derived from MODIS and Landsat 7 ETM+ data has been done. Main goal is to understand how effective MODIS images can be for vegetation characterization on large areas, as compared to the Landsat 7 ETM+ ones.
In this paper a methodology is proposed with the aim of measuring the difference between NDVI values derived from the two different data, considering synthetic parameters and investigating their dependency on the geometric resolution of the images.
Great attention was paid to the problem of the geometric co-registration of the two types of data. This is a very sensitive parameter for the subsequent analysis. A mixed approach was adopted: images were firstly orthoprojected to eliminate sensor geometry and relief displacement effects; subsequently, a refining image-to-image co-registration procedure was carried out through a homographic transformation implemented in a self-developed routine. Two pairs of contemporary images (MODIS and Landsat 7) were used as benchmarks for our tests. Simplified procedures aimed at calibrating images and at removing atmospheric noise were performed. The resulting corrected images were used to calculate NDVI images. These ones (two pairs) were then compared through a statistical approach in order to investigate how a different geometric resolution can influence the NDVI values.
The proposed approach is not a traditional image based (matrix comparison) but a new one. NDVI value correspondences were considered between the MODIS pixel and the group of Landsat pixels belonging to the polygon which represents the considered MODIS pixel in the Landsat image space. Statistics extracted on-the-fly from these Landsat pixels were used to investigate in depth the relationship between them and NDVI value of the corresponding MODIS pixel. NDVI differences were calculated between the single NDVI MODIS values and a synthetic parameter (mean value) of the homologous Landsat pixel group. A direct comparison between the NDVI values obtained from MODIS and Landsat 7 images has shown a systematic error that can be read as bias (MODIS NDVI over estimation). This led the authors to determine a suitable model in order to eliminate the bias, whose presence would have conditioned later comparisons. Original MODIS image was then corrected through the defined model. This has been designed to be suitable for any MODIS image acquired over the same area (parameterization was used). New NDVI differences were calculated using the corrected MODIS images and the previous Landsat 7 ones.
In order to investigate the nature of the residual differences and to try to recognize the critical MODIS pixels, some considerations were made concerning the statistics of each corresponding group of Landsat pixels. A classification of the MODIS pixel was generated according to the behaviour of their differences with respect to the adopted statistics.

1. RESEARCH GOAL

This study is part of a research project aimed at evaluating which limits and potentialities result from the use of low resolution MODIS data for hydrological purposes, such as support to water balance projects in river basins with little available ground data. This is of great importance, for instance, in large areas of developing countries, where hydrological monitoring alone cannot allow comprehensive studies on long-term water balance. In this context, continuity of available data as guaranteed by the MODIS platform is an important requirement (see e.g. Gallo et al., 2005; Kurtis et al., 2003). If the areas of interest are of the order of a few hundreds of km^2 it is also important to have an evaluation of the quality of the MODIS representation
of variables of hydrological interest, such as vegetation. A way to afford this task is to refer to higher resolution sensor in a coarse-resolution approach (see e.g. Oleson et al, 1995). In this case, comparison has been made between MODIS and Landsat 7 data. A wider use of MODIS can be considered a sensitive matter also:

a) because of the currently operational limitations of Landsat 7 (slc-off acquisitions);
b) because of the greater economic convenience of the MODIS data (they are free);
c) because of the higher data frequency of MODIS.

In particular, considering vegetation properties, the main task of this work was that of comparing of NDVI images derived from Terra MODIS and Landsat 7 ETM+ data, respectively.

2. DATA AND TEST AREA

Two pairs of contemporary images, acquired by the sensors Terra - *MODIS* (*Moderate Resolution Imaging Spectrometer)* and Landsat 7 *ETM+* (*Enhanced Thematic Mapper*) respectively were considered.
The test area is a portion of the northern coast of Sicily (Italy), as shown in Figure 1. It was chosen mainly because of the great variety of vegetation and other land covers that can be encountered. Considering MODIS images, the product named "*MODIS/Terra Calibrated Radiances 5-Min L1B Swath 250m*"

(MOD02QKM) was selected for this study (Toller, 2003; Barbieri, 1997). Level 1B images represent calibrated and geolocated data for MODIS spectral bands 1 and 2. The MODIS data were obtained completely free of charge on the WWW from the EDG (*EOS Data Gateway*).
As far as ETM+ images are concerned ESA CEOS data were acquired for the study. Two datasets (each containing one MODIS and one ETM+ image) were prepared considering two similar summer dates of different years (02/08/2000, 07/07/2002).

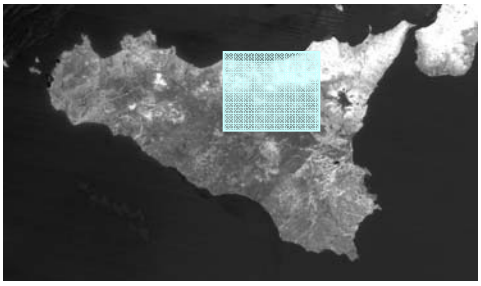

Figure 1. Test area

These datasets were forced to assume the same size in order to make the results comparable.
The basic features of the two sets of data are shown in Table 1.

	Terra-MODIS	**Landsat7-ETM+**
Bandwidth specifications	*Band 1: 620-670nm* *Band 2: 841-876 nm*	*Band 3: 630-690 nm* *Band 4: 780-900 nm*
Spatial resolution	*250 m*	*30 m*
Radiometric resolution	*12 bits*	*8 bits*
Data Frequency	*2 days (global coverage)*	*16 days (seasonal global coverage capability)*

Table 1. Basic features of MODIS and ETM+ data.

As required by the goal of the research, four NDVI (*Normalized Difference Vegetation Index*) images (2 ETM+ and 2 MODIS) were derived from these data:

$$NDVI = \frac{NIR - R}{NIR + R} \qquad (1)$$

where: R = *Red channel*
NIR = *Near InfraRed channel*

NDVI varies between -1 and + 1. Due to its 'ratioing' properties, the NDVI cancels out a large proportion of signal variations attributed to calibration, noise, and changing irradiance conditions that accompany changing sun angles, topography, clouds/shadow and atmospheric conditions.

3. DATA COMPARISON PROCEDURE

3.1 Overview

In order to compare MODIS and Landsat NDVI values, the images were preventively radiometrically preprocessed and co-registered. The radiometric calibration of the Landsat data was carried out to convert sensor DNs (*Digital Numbers*) to at-the-sensor reflectances; the atmospheric correction was successively performed for both data through the simplified Dark Subtraction approach. Solar and topographic correction was ignored since NDVI is a ratio in which multiplying factors can be neglected.
Image co-registration was done following the procedure shown in section 3.2.

3.2 Image dataset co-registration

While evaluating, from an operational point of view, two different types of data (*MODIS* and *Landsat 7*) great attention has to be paid to their co-registration. It should be pointed out that by co-registered images we intend geometrically coherent images, that is images whose pixels are homologous to each other. Any consideration about image radiometry is greatly conditioned by the "goodness" of such an operation. The basic idea is to find a suitable relationship between the Landsat 7 sample grid and the MODIS one, in order to understand and measure the resulting differences. Even though the Landsat 7 and Terra satellite orbits are the same, the images acquired by ETM+ and MODIS sensors appear to be quite different, geometrically speaking; it is not an easy task to force one image to perfectly fit the other one. In order to reach an appropriate degree of correspondence, this problem was considered in great detail. Firstly, a preliminary evaluation of the relative positioning error (*RPE*) due to the relief displacement problem (the test area presents relief heights ranging from about 0 up to 1800 m) was carried out, following the operational scheme of figure 2.

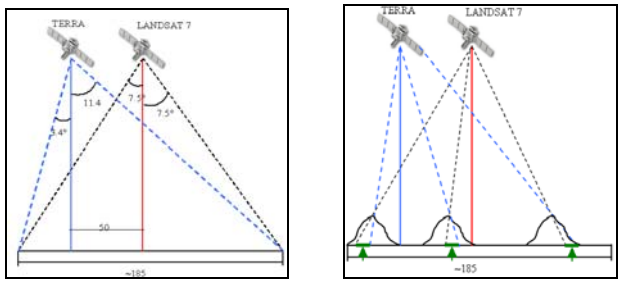

Figure 2. (Left) Satellite acquisition scheme; (Right) Relative Positioning Error variation over the scene (Landsat 7 image swath) due to relief displacement.

The mean distance between the satellite ground tracks were estimated to be about 50 km, according to the footprints of the images, as communicated by the metadata files.
Considering the size of the Landsat 7 image footprint, the correspondent RPEs were evaluated for different height values (H = 2000, 1000, 500 m). The results of Table 2 show that a simple approach based on a flat image-to-image transformation cannot be adopted to co-register images.
An orthocorrection process was therefore carried out for both images to keep co-registration errors low.

Height (m)	**RPE min (m)**	**RPE min (n. pixel Landsat)**	**RPE max (m)**	**RPE max (n. pixel Landsat)**
2000	*141*	*4.7*	*162*	*5.4*
1000	*70*	*2.3*	*81*	*2.7*
500	*35*	*1.2*	*41*	*1.4*

Table 2. RPEs vs Height values

A Digital Elevation Model with a 50 m grid step and an estimated height accuracy of about 2.5 m was used to produce orthoimages. 10 Ground Control Points (GCPs), extracted from

a vector map (scale 1:25:000) of the Sicily coastline were used to assign a National Reference System to the image (ED 50 UTM 32N).
The Landsat 7 images were corrected using OrthoEngine PCI Geomatics 9.0 software which is equipped with the rigorous Landsat model. The final orthoimages (2000 and 2002) estimated accuracy is about 0.7 Landsat pixels (that is, about 20 meters) according to the calculated Root Mean Square Error (RMSE) for both images.
MODIS bands 1 and 2 were corrected through a 1st order Rational Function Model (RFM). The resulting RMSE was about 0.45 MODIS pixels (that is, about 112 m) for both the 2000 and 2002 images.
In order to guarantee a better co-registration between the images, a further image-to-image registration procedure was applied to the obtained orthoimages. Some tests showed that the usual flat correction models (polynomials, triangulation, spline) were not sufficiently good, generating RMSE of about 4 Landsat pixels.

$$c_L = \frac{A_1 \cdot c_M + A_2 \cdot r_M + A_3}{A_4 \cdot c_M + A_5 \cdot r_M + 1}$$
$$r_L = \frac{A_6 \cdot c_M + A_7 \cdot r_M + A_8}{A_4 \cdot c_M + A_5 \cdot r_M + 1} \quad (2)$$

where: $\mathbf{A_i}$ = model parameters
$\mathbf{c_L}$,$\mathbf{r_L}$ = Landsat image coord.
$\mathbf{c_M}$, $\mathbf{r_M}$ = MODIS image coord.

This has forced the authors to develop a specific routine for the task. A homography transformation (HT1) was implemented (*IDL, Interactive Data Language* programming tool) relating the Landsat image coordinates (base image) to the MODIS one (warp image), as stated in (2).
Due to the great difference between the geometric resolution of the two types of data, there was a great uncertainty in the identification of suitable Ground Control Points, especially over the MODIS image, where the exact point correspondent to the one collimated over the Landsat image (30 m resolution) can float inside a larger window (the MODIS pixel).
In order to reduce this effect over the HT1 RMSE, considering that the implemented HT1 is calibrated using sub-pixel image coordinates, a specific collimation refining procedure was developed and applied before HT1. This procedure estimates the inverse HT (HT2) relating the MODIS image coordinates (base image) to the Landsat ones (warp image), (3).
According to the residuals obtained from the Least Squares HT2 model parameter estimation, decimal digits of the collimated MODIS image coordinates (c_M, r_M) are moved to lower the RMSE, while the Landsat image coordinates remain the same.

$$c_M = \frac{B_1 \cdot c_L + B_2 \cdot r_L + B_3}{B_4 \cdot c_L + B_5 \cdot r_L + 1}$$
$$r_M = \frac{B_6 \cdot c_M + B_7 \cdot r_M + B_8}{B_4 \cdot c_L + B_5 \cdot r_L + 1} \quad (3)$$

where: $\mathbf{B_i}$ = model parameters
$\mathbf{c_L}$,$\mathbf{r_L}$ = Landsat image coord.
$\mathbf{c_M}$, $\mathbf{r_M}$ = MODIS image coord.

This operation produces new corrected MODIS image coordinates for the Ground Control Points, which are then used to estimate HT1 parameters.

The computed RMSEs are shown in table 3 and they represent the final co-registration errors that were accepted.

2000 dataset RMSE (Landsat pixels)	2002 dataset RMSE (Landsat pixels)
1.82	2.21

Table 3. RMSEs obtained after co-registration for the two datasets.

The entire comparison process, that is presented later on, is based on the following co-registration approach. It operates by calculating the correspondent floating point Landsat image coordinates for the 4 corners of each MODIS pixel.

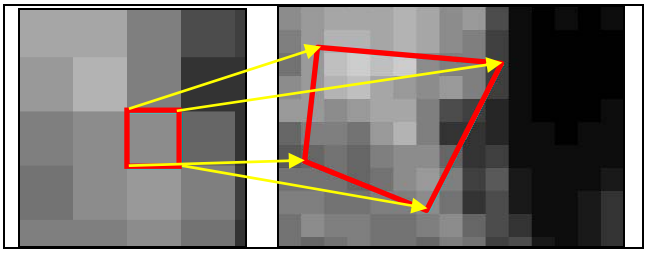

Figure 3. Homography model. The self-developed procedure operates by transforming the corners of each MODIS pixel into the Landsat image space.

For each MODIS pixel can be therefore defined a polygon ($P_{landsat}$) in the Landsat space, that includes several Landsat pixels (figure 4). These ones are considered to contribute to the total reflectance which is recorded as a single value by the MODIS CCD (*Charge Coupled Device*). The comparison proceeds considering the statistical distribution of the DN of these Landsat pixels with the single DN obtained from the original homologous MODIS pixel.

3.3 Spectral comparison

The NDVI comparison was carried out according to the following two steps:
a) the first (statistical survey) was devoted to the quantification of the local differences between the NDVI values;
b) the second was devoted to the assessment of the nature of the resulting NDVI differences and to the identification of those MODIS pixels that can be considered critical for the potential substitution of Landsat derived NDVI with the MODIS ones. The features related to the radiometric homogeneity of the MODIS pixels were investigated in particular.

3.3.1 Statistical survey of NDVI differences

The previously described geometric correction procedure allows each MODIS NDVI pixel to be linked to the correspondent distribution of the NDVI Landsat pixels that belong to the $P_{Landsat}$ polygon. This has to be represented by synthetic statistical parameters that can allow the comparison to be made. Sensor recording mode suggested the choice. During the acquisition process, the sensors integrate the radiation from the ground area (IFOV area), defined by the IFOV (*Istantaneous Field of View*) and code it as a single discrete value (DN). DN can therefore be considered as the result of the sum of energy reflected by all the objects that belong to the IFOV area; these objects participate in the signal, according to their different spatial distribution inside the IFOV area itself. This would suggest to calculate, for each $P_{Landsat}$ polygon, some

statistical parameters, suitable to describe the global spectral behaviour of the pixels included in the polygon. The considered parameters are: mean μ_{NDVI_L}, median Md_{NDVI_L} and standard deviation σ_{NDVI_L} of the NDVI values obtained from each $P_{Landsat}$. A first analysis was carried out to verify the possible existence of a relationship between the statistical distribution of the MODIS NDVI values (single pixels) and the statistical distribution of the mean Landsat NDVI values calculated for each $P_{Landsat}$. The *Pearson linear correlation coefficient* was therefore calculated. The $R_{X,Y}$ values are ≥ 0.9 for both the considered datasets (2000 and 2002). The existence of a relationship between the two populations has therefore been demonstrated. This was a basic condition and requirement for the subsequent tests. In order to quantify the NDVI differences for each dataset, the following quantities were calculated:

$$\Delta_{LM_1} = \mu_{NDVI_L} - NDVI_M$$
$$\Delta_{LM_2} = Md_{NDVI_L} - NDVI_M \qquad (4)$$

where: $NDVI_M$ = MODIS NDVI value for generic pixel i; μ_{NDVI_L}, Md_{NDVI_L} = mean and median values calculated for the corresponding $P_{Landsat}$.

This concept for NDVI difference computation is illustrated in figure 4. Taking into account the kind of vegetation that covers this quite arid area it was assumed sufficient to consider the range of NDVI values (the NDVI values were related to the Landasat data) between -0.2 and 0.8. A total of 20 $NDVI_L$ classes of width equal to 0.05 were identified within this range. The differences Δ_{LM} were assigned to the relevant classes through the control, for every $P_{Landsat}$, of the $NDVI_L$ class, where its mean value μ_{NDVI_L} was included.

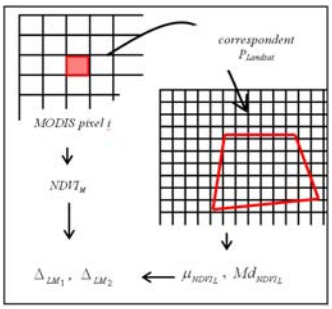

Figure 4. NDVI difference (Δ_{LM}) computation scheme based on the polygon approach.

The mean $\overline{\Delta_{LM\ i}}$ of the obtained difference values was calculated for each class. Figure 6 shows the trends of the differences $\overline{\Delta_{LM\ i}}$ respect to $NDVI_L$ value for the two observation periods (2000 and 2002). It is possible to notice a relationship between the two observed variables that can be approximated (at least for $NDVI_L$ values > -0.25) with linear functions represented by the equations stated in figure 5.
The linear relationships (confirmed with the high values of the R^2 coefficient), show similar (invariant?) *GAINS* and different *OFFSETS* for the two periods.
It is worth to underline that linear regression parameters estimation was conducted without taking care about the number of observations (Δ_{LM}) of each NDVI class in order to generate a correction tool suitable for all the NDVI values. If weights had been used, regressions would have certainly been conditioned by the largest classes.
Further research is at present performed with the aim of verifying whether these observed systematic differences can be related to specific critical states of the calibration algorithms used by the distributors of MODIS imagery, or to some limits of the applied simplified atmospheric correction models.

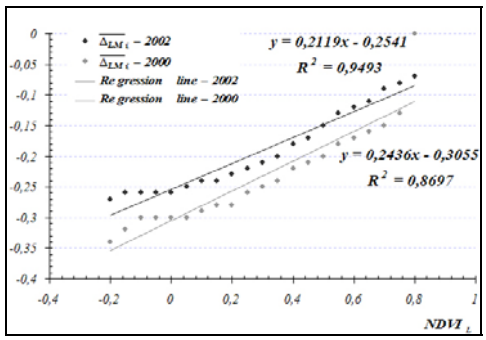

Figure 5. Trends of the difference means $\overline{\Delta_{LM\ i}}$ respect to $NDVI_L$ value for the two observation periods and pertinent interpolation lines.

The identification of linear relationships allowed the observed bias from NDVI MODIS image to be removed. This was necessary for the evaluation of the residual differences which were closely connected to the different *Ground Sample Distance* (GSD) of the two types of data. This correction (matrix operation over the NDVI MODIS image) was applied as it follows:

$$NDVI'_M = NDVI_M + C_{NDVI} \qquad (5)$$

where: $NDVI_M$ = MODIS NDVI value for pixel i;
C_{NDVI} = correction value estimated by linear regression.

Using the corrected NDVI MODIS images, new differences were calculated as previously between the NDVI values (figure 4). The distribution of the obtained difference values was again analysed respect to the previous $NDVI_L$ classes. The new results are illustrated in figures 6 and 7.

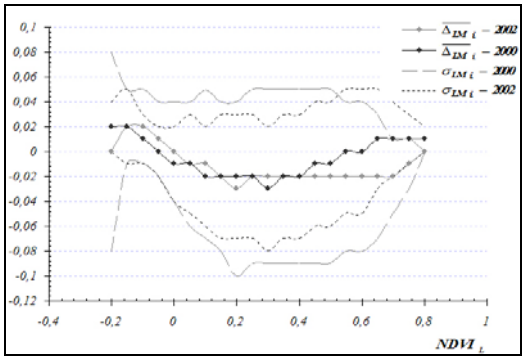

Figure 6. Trends of the new differences $\overline{\Delta_{LM\ i}} \pm \sigma_{LM\ i}$ respect to $NDVI_L$ value for the two observation periods.

Figure 6 shows how the situation has changed quite remarkably; the proposed dependency trends (between the distributions of the differences $\overline{\Delta_{LM\ i}}$ and the distribution of the $NDVI_L$ classes) would seem to exclude any correlation, thus suggesting the absence of any further systematism. Furthermore, the observed

differences settle on values of about zero which are however lower than the corresponding standard deviations $(\sigma_{LM\,i})$.

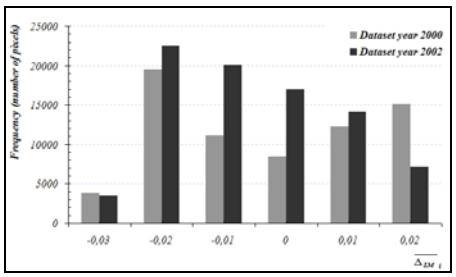

Figure 7. Histograms of the distributions of $\overline{\Delta_{LM\,i}}$ for the datasets relative to the years 2000 and 20002.

3.3.2 Critical MODIS pixel mapping

The possible dependence of the encountered differences on the radiometric homogeneity conditions of the $P_{Landsat}$ corresponding to the MODIS pixels was investigated on the basis of the indications obtained during the previous stage.
The statistic distribution of the NDVI Landsat values of each $P_{Landsat}$ pixels was analysed to verify whether one of the following characteristic situations could occur:

- the pixels belonging to $P_{Landsat}$ corresponding to the considered MODIS pixel have a mean value μ_{NDVI_L} that falls into the class of NDVI to which the absolute majority (> 50%) of the pixels of $P_{Landsat}$ belongs. These MODIS pixels are those that are characterised by radiometric homogeneity. A reduced difference between the NDVI values is expected for this type of pixels (hereafter referred to as *Type A* pixels);
- the pixels belonging to $P_{Landsat}$ corresponding to the considered MODIS pixel have a mean value μ_{NDVI_L} that falls into a different NDVI class from that to which the absolute majority (> 50%) of the pixels of $P_{Landsat}$ belongs. In this case, we are dealing with MODIS pixels whose behaviour has to be verified (hereafter referred to as *Type C* pixels);
- the pixels belonging to $P_{Landsat}$ corresponding to the considered MODIS cell have a mean value of μ_{NDVI_L} which is a result of the joint contribution of groups of pixels belonging to different NDVI classes, none of which represents the absolute majority of the pixels of $P_{Landsat}$. These MODIS pixels are mixed and constitute the expected critical element introduced by the different geometric resolutions of the two sensors. These MODIS pixels are hereafter referred to as *Type B* or "mixed". (an example is given in figure 8, showing the correspondent histogram of a *Type B* $P_{Landsat}$ polygon).

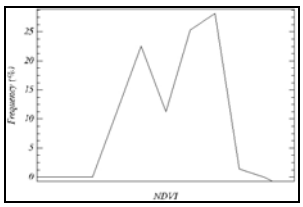

Figure 8. Histogram of the relative frequencies (% of the total pixels contained in $P_{Landsat}$).

The previously illustrated conditions were verified within a range of $NDVI_L$ values between -0.2 and +0.8 (0.1 amplitude classes). It was possible to assign each MODIS pixel to one of the three previously defined classes (A, B or C) and to generate the MODIS classified images corresponding to the two investigated periods.
The percentage incidence of the 3 types of classes on the total of the MODIS image pixels, relative to the examined dataset, is summarised in figure 9. As can be seen, *Type A* MODIS pixels prevail in the dataset relative to the year 2002, while *Type B* MODIS pixels prevail in the dataset relative to the year 2000. The *Type C* MODIS pixels seem to have a similar incidence for both years that were examined. Such information can be used to estimate the potential "expected" error that can be ascribed to the adoption of the MODIS data instead of the Landsat one. It is believed that it can in fact be concentrated on *Type B* pixels.
A joint analysis has made it possible to evaluate the existence of a relationship between the distribution of the Δ_{LM} residual difference population and the typology of the MODIS pixels. The graphs shown in figures 10 and 11 illustrate the Δ_{LM} histograms for the three considered types. The data summarised in the diagrams refer to the complete datasets, including the pixels with values of NDVI outside the considered range.
It can be seen that for the majority of cases, the residual differences have a frequency maximum (mode) in correspondence to the values close to zero for all the types of pixels examined. A prevalence of *Type A* MODIS (or homogeneous) pixels can be observed for difference values close to zero, as expected.
The contribution of the total distribution given by the *Type B* (or mixed) pixels instead become more important for the values of the increasing Δ_{LM} differences (absolute value).
According to the purposes of vegetation characterisation of the territory useful for hydrological applications, the following residual difference values were considered critical: $|\Delta_{LM}| > \mathbf{0.1}$.

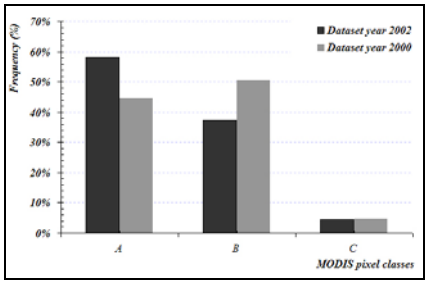

Figure 9 Percentage distribution of the three types of MODIS pixels relative to the examined datasets.

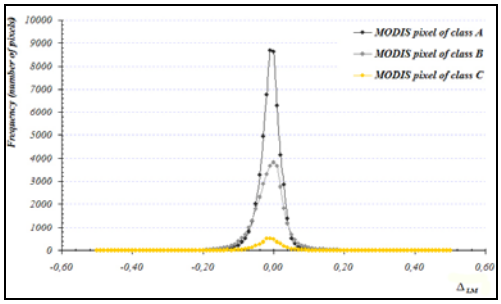

Figure 10. Histograms of Δ_{LM} for the 2002 dataset.

The homogeneity characteristics of the MODIS pixels exceeding the stated threshold were therefore investigated. The results of these analyses are given in table 4.

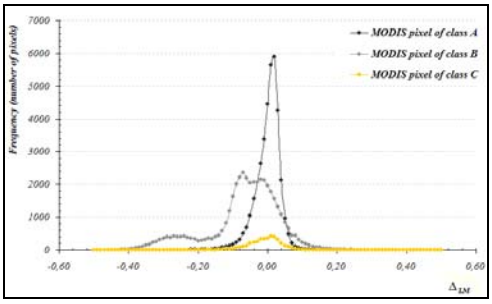

Figure 11. Histograms of Δ_{LM} for the 2000 dataset..

As can be seen, the critical MODIS pixels represent a minor percentage of the total scene. It can also be observed how the critical difference values are connected, in most cases, to the presence of *Type B* MODIS pixels. Furthermore, it should also be observed how a certain percentage of the MODIS pixels that show acceptable residual difference values are still of *Type B*, even if unexpected. The critical MODIS pixels ($|\Delta_{LM}| > 0.1$) were finally identified on the MODIS image in order to examine their spatial distribution (figure 12).

2000	**Pixels with** $\|\Delta_{LM}\| > 0.1$	14.25% of the total	type A type B type C	5.33% 92.92% 1.75%
	Pixels with $\|\Delta_{LM}\| < 0.1$	85.75% of the total	type A type B type C	51.04% 43.59% 5.36%
2002	**Pixels with** $\|\Delta_{LM}\| > 0.1$	2.64% of the total	type A type B type C	30.60% 62.68% 6.73%
	Pixels with $\|\Delta_{LM}\| < 0.1$	97.36% of the tota	type A type B type C	59.07% 36.64% 4.29%

Table 4. Distribution of critical MODIS pixel types.

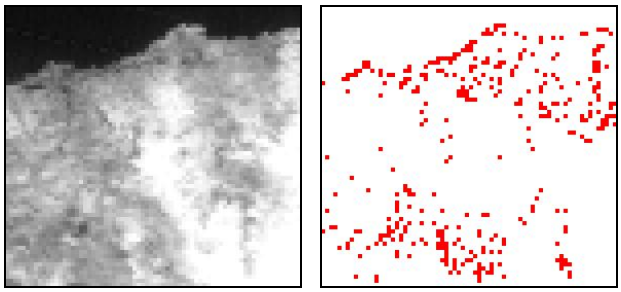

Figure 12. MODIS critical pixels $|\Delta_{LM}| > 0.1$ mapped over the scene (an example subset).

4. CONCLUSIONS

The conducted analyses were addressed to the determination of the degree of substitutability of the NDVI Landsat-derived with the equivalent MODIS one. These analyses have shown that:

- the NDVI images derived from the MODIS acquisitions show a systematic difference with respect to the corresponding Landsat acquisitions that can be modelled;
- the NVDI MODIS images, once corrected of the aforementioned systematic differences, guarantee a good homogeneity of values with the NDVI Landsat images;
- the greater differences of the NVDI values respectively generated from the two types of data can be recognized above all in the mixed cells (*Type B*);
- the greater errors result to be lower (in terms of number of pixels) than the expected value (all the *Type B* pixels).

The comparison between the two types of data is greatly conditioned by the type of co-registration approach that is adopted. It can be considered that the proposed procedure guarantees a sufficient homology between the compared scenes and it is certainly higher than that which can be obtained using simple planar transformations. According to such results, we intend to proceed with a more detailed investigation of the systematic difference between MODIS and Landsat NDVI: many other case studies have to be considered before such a problem can be defined as “typical”.
It would be interesting, furthermore, to look at the impact of the Point Spread Function in the found bias.
Currently we are working to develop a MODIS image resampling procedure based on geometric information obtained from a static land cover classification map, which will be useful to virtually increase the MODIS geometric resolution, reducing the gap between the two data. This procedure will permit the degree of substitutability of the Landsat data with the MODIS one to be improved as far as the NDVI computation is concerned.

ACKNOWLEDGEMENTS

This work has been supported by funds from Italian Ministry of Education and Research (MIUR COFIN 2003). Thanks are due to Goffredo La Loggia for providing the Landsat data.

REFERENCES

Toller G.N., Isaacman A., 2003. *MODIS Level 1B Product User’s Guide*. MCST (MODIS Characterization Support Team) for NASA/Goddard Space Flight Center Greenbelt.

Barbieri R., Montgomery H., Qiu S., Barnes B.,1997. *MODIS Level 1B Algorithm Theoretical Basis Document*. MCST (MODIS Characterization Support Team) Algorithm Development Team.

Kurtis J. Thome, Robert A. Barnes, and Gene C. Feldman, 2003, *Intercomparison of ETM+, MODIS, and SeaWiFS using a land test site*, Proceedings of SPIE, Volume 4881 - Sensors, Systems, and Next-Generation Satellites VI, Hiroyuki Fujisada, Joan B. Lurie, Michelle L. Aten, Konradin Weber, Editors, April 2003, pp. 319-326.

Gallo K., Lei Ji, Reed B., Eidenshink J., Dwyer J., 2005, *Multi-platform comparisons of MODIS and AVHRR normalized difference vegetation index data,* Remote Sensing of Environment 99, pp. 221 – 231.

Oleson, K.W., S. Sarlin, J. Garrison, S. Smith, J.L. Privette, and W.J. Emery, 1995: Unmixing multiple land-cover type *reflectances from coarse spatial resolution satellite data*, Remote Sensing of Environment 54, pp. 98-112.